XLVI CILAMCE
VITÓRIA - ES - BRAZIL - 2025
XLVI IBERO-LATIN AMERICAN CONGRESS ON COMPUTATIONAL METHODS IN ENGINEERING

Computational Modeling of Fiber-Reinforced Cementitious Matrices

Lucca R.P. Borges[1], Daniel de L. Araújo[1], Arthur A.A. Albuquerque[1]

[1]*Escola de Engenharia Civil e Ambiental, Universidade Federal de Goiás*
Av. Universitária, Q. 86, Lote Área 1488, 74605-220, Goiânia/Goiás, Brazil
luccaptc@discente.ufg.br, dlaraujo@ufg.br, arthuralax@ufg.br

Abstract. *Various studies have been conducted to expand knowledge of the structural behavior of fiber-reinforced concrete (FRC), making it as a potential alternative to conventional reinforced concrete in specific applications. The addition of fibers to the concrete matrix primarily enhances the tensile behavior of plain concrete, improving its resistance to bending and shear forces, as well as its ductility and toughness. These characteristics are directly related to the fact that once fibers are embedded and bonded to the cementitious matrix, they hinder the initiation and propagation of cracks. A common strategy for investigating the behavior of FRC under bending and shear forces is numerical simulation using the Finite Element Method (FEM). The approach used here explicitly models the fibers as finite elements randomly dispersed within the continuous domain of the concrete. The primary objective is to evaluate the influence of the fiber-matrix interaction on the composite's response by numerically simulating of a series of experimental tests carried out using the commercial FEM software DIANA FEA®. The results show that the response of the numerical model depends on the properties of the fiber-matrix interface used, as well as on the way the fibers are generated.*

Keywords: Steel-Fiber Reinforced Concrete, Computational Modeling, Non-Linear Analysis, Fiber-Matrix Interaction, Finite Elements.

1 Introduction

Fiber-reinforced concrete (FRC) is a composite that can be used in some situations as an alternative to reinforced concrete, especially in structures subject to shear force. The addition of fibers embedded in the cementitious matrix contributes to improving the tensile behavior of plain concrete, not only by increasing the material's resistance to bending and shearing stresses but also by increasing its ductility and toughness. The interaction at the interface between the fiber and the cementitious matrix is of special importance for simulating the behavior of this composite when subjected to bending and shear stresses. In addition, it has been found that the concrete's strength and the percentage of fibers also influence the final strength of the FRC.

According to Khaloo and Kim [1], as concrete strength increases, the composite's shear strength also increases. This occurs due to an increase in the bond strength at the fiber-cementitious matrix interface. Studies conducted by Ahmed and Chidambaram [2] show that parameters such as the minimum percentage of fibers in the composite can influence the failure mode of the material under bending and shear stresses. Currently, there are both numerical and analytical methods that attempt to simulate the structural behavior of FRC. Lee and Foster [3] present an analytical model called Variable Engagement Model II (VEMII), developed from data from direct shear tests on fibers. Lee, Cho, and Vecchio [4] also developed a model called the Diverse Embedment Model (DEM), capable of predicting the tensile behavior of FRC, which can be applied to both concrete containing hooked fibers and concrete with straight fibers.

Given the importance of the topic, the main objective of this work is to numerically evaluate the strength of matrices reinforced with steel fibers. To achieve this objective, three tests previously simulated by Bittencourt Jr. [5] are modeled and numerically simulated here, but using the DIANA FEA® [6] finite element software. This work first performs the numerical simulation of fiber pull-out tests to analyze the influence of the fiber's embed-

ment length in the matrix. Subsequently, a direct tensile test is simulated, considering both modeling with intersecting fibers and modeling with non-intersecting fibers.

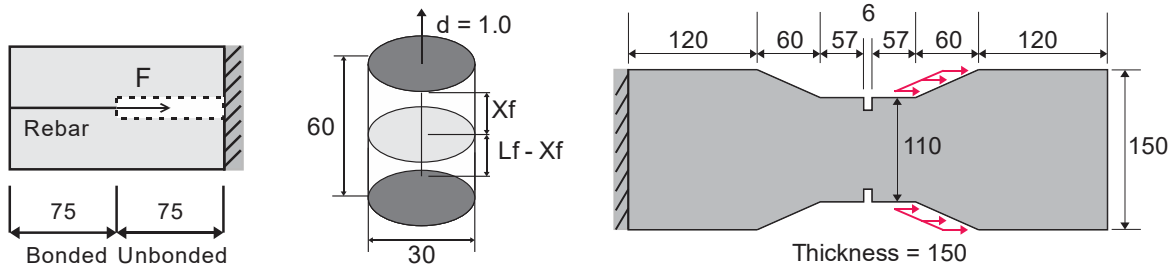
2 Computational tests performed

To achieve the proposed objectives, two fiber pull-out tests (Tests A and B) and one direct tension test (Test C) were modeled and simulated, as shown in figure 1. Tests A and B represent the pull-out of a steel fiber embedded in a cementitious matrix. In Test A, the reinforcement is a 10 mm diameter bar, while in Test B, a steel fiber with a 0.565 mm diameter and 30 mm length is used. In the first case, the force is applied directly to the end of the bar until the bar-matrix interface fails. In the second case, the force is applied to the top face of the cylinder until a 1 mm displacement is reached. To analyze the influence of the fiber embedment length, five different lengths (Xf) were adopted in Test B. In this case, the fiber length in one half of the cylinder is Xf, while the remaining length in the other half is the difference between the total fiber length (Lf) and Xf. The five values adopted for Xf in this test are: 15 cm, 12 cm, 9 cm, 6 cm, and 3 cm.

The direct tension test, Test C, consists of a specimen with a variable cross-section. The specimen has two notches, one at the top and one at the bottom, at the cross-section with the smallest height (110 mm). This test simulates the behavior of a composite reinforced with steel fibers of 1.05 mm diameter and 50 mm length under tensile stress. As this model involves multiple fibers dispersed in the matrix, two simulations were performed: one allowing fiber intersection and another considering non-intersection during the fiber generation process.

For the random generation of non-intersecting fibers, the fiber generation algorithm provided by Al-Rumaithi [7] for the MatLab programming platform was used. The algorithm generates fibers at random positions within a rectangular region. To do this, the user must provide the number of fibers to be generated, the dimensions of the region, and the fiber length. The "rand" function in MatLab is used to randomly generate the central coordinates of the fibers and their angle. After each fiber is generated, it is checked to ensure it does not intersect previously generated fibers and that its end coordinates are within the initially defined region. If, during a generation, one of these conditions is not met, the fiber is discarded, and the process is restarted for that fiber until it meets all imposed conditions

For Test C, the presence of 300 fibers was considered, which corresponds to approximately a 0.5% fiber volume. This quantity was determined from the central volume of the specimen and distributed in an area of 180 mm x 110 mm. Subsequently, the algorithm was modified by removing the restriction that fibers could not intersect during generation, while maintaining only the restriction that their ends must be contained within the delimited area.



(Test A) (Test B) (Test C)

Figure 1 – Representation of the simulated tests: (Test A) Pull-out test of a bar in a prismatic plane specimen, (Test B) Fiber pull-out tests in a cylindrical specimen, and (Test C) Direct Tension Test. Units in mm.

3 Constitutive Models and Finite Elements

DIANA FEA® [4], a finite element software, was used to perform the numerical simulations. In all simulations, the fibers were represented by a perfect elastoplastic constitutive model. "Reinforcement" finite elements were used, which allows for the creation of a separate mesh for the dispersed fibers independent of the cementitious matrix mesh. For Tests A, B, and C, the elastic moduli adopted for the fibers were 207 GPa, 210 MPa, and 200 GPa, respectively, while the yield stress was 555 MPa, 345 MPa, and 520 MPa, respectively. In all models, a Poisson's ratio of 0.3 was used.

For the cementitious matrix in simulations of Tests A and C, the T6MEM finite element was used. This is a 3-node, linear isoparametric triangular plane element with a single integration point for solving element integrals. In the 3D model of Test B, the TP18L finite element, a 6-node linear isoparametric element, was employed. The fibers (and the bar in Test A) were modeled using a truss-type finite element, which has degrees of freedom only for displacements. The software automatically considers a zero-thickness interface element to represent the fiber-matrix interaction, to which normal and tangential stiffnesses are assigned.

The numerical method used to solve the linear system of equations in all simulations was the Quasi-Newton (BFGS) method, also known as the Secant method. According to the DIANA FEA® User Manual [4], this method uses information from previous solution vectors and unbalanced force vectors during an increment to obtain a better approximation for the solution.

In the models for Tests A and B, the cementitious matrix was simulated with linear elastic behavior, as the focus of these tests was to evaluate the relationship between the shear stress at the fiber-matrix interface and its slip. The elastic modulus and Poisson's ratio were 30 GPa and 0.2, respectively.

For the Test C model, the elastic modulus and Poisson's ratio used for the cementitious matrix were 18.10 GPa and 0.23, respectively. To represent the non-linear behavior of the cementitious matrix, the Total Strain Crack model with Rotating Crack Orientation was adopted. The non-linear tension softening model proposed by Hordijk, Cornelissen & Reinhardt [8] was used, with a tensile strength (ft) and fracture energy (Gf) of 1.72 MPa and 0.100 N/mm, respectively.

All these tests were previously simulated by Bittencourt Jr. [5]. For his simulations, the author proposed two constitutive relationships, shown in equations (1) and (2), to represent the bond-slip relationship. In the numerical simulation of Test A, the author used equation (1) with the following parameter values: s1=s2=0.6 mm, α=0.4, s3 =1.0 mm, τf=1.5 MPa, and τmax=10 MPa.

$$\tau\ s\ = \begin{cases} \tau_{\max}\left(\dfrac{s}{s_1}\right)^{\alpha} & \text{if}\ \ s \le s_1 \\ \tau_{\max} & \text{if}\ \ s_1 \le s \le s_2 \\ \tau_{\max} - \dfrac{\tau_{\max} - \tau_f \quad s - s_1}{s_2 - s_1} & \text{if}\ \ s_2 \le s \le s_3 \\ \tau_f & \text{if}\ \ s > s_3 \end{cases}. \tag{1}$$

Equation (2) was used to represent the bond-slip relationship in the numerical simulation of Test B. The parameter values used in this equation were: s1 = 0.1 mm, τmax = 3 MPa.

$$\tau\ s\ = \begin{cases} \tau_{\max}\left(\dfrac{s}{s_1}\right) & \text{if}\ \ s \le s_1 \\ \tau_{\max} & \text{if}\ \ s > s_1 \end{cases}. \tag{2}$$

To numerically represent the bond-slip relationship in Test C, Equation (1) was also used. The following values were used for the curve parameters in this simulation: s1=s2=0.01 mm, α=0.4, s3=3.5 mm, τf=1.5 MPa, and τmax=6.5 MPa.

For the representation of the linear elastic behavior of the fiber-matrix interface, the stiffness values suggested by Bittencourt Jr. [5] were adopted: 103 N/mm³ for normal stiffness and 109 N/mm³ for tangential stiffness.

4 Simulations and results analysis

Figure 2 shows the generated meshes for the three simulated tests. To represent the cementitious matrix, meshes with 130, 192, and 2,326 finite elements were used for Tests A, B, and C, respectively. The fibers are represented by the elements in yellow.

For the Test C simulations, the fiber distribution was limited to the central region. This consideration was made to reduce processing time and memory costs in the FRC simulations, as the crack in this test occurs in the notched region. Tests A and C were modeled considering a plane stress state, while Test B was represented in 3D.

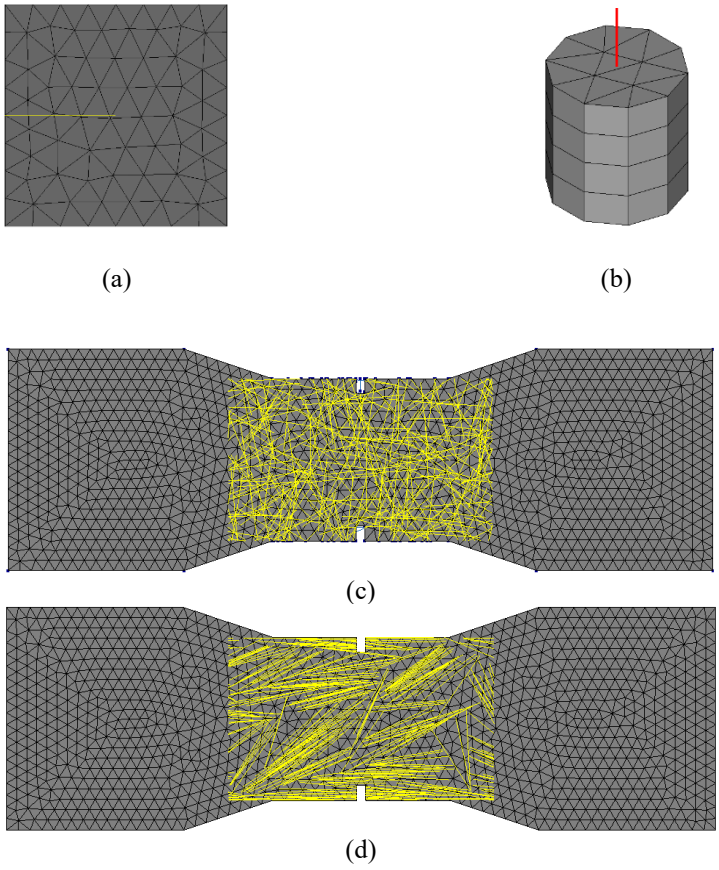


Figure 2 – Meshes of the Finite Elements Adopted in the Simulations. (a) Test A, (b) Test B, (c) Test C with intersecting fibers, and (d) Test C with non-intersecting fibers.

Figure 3 shows that the Tension Stress versus Slip curve obtained from the numerical simulation in DIANA FEA® [6] exhibits the same behavior as the curves determined from the bond-slip relationship (Equation (1)) and Bittencourt Jr.'s [5] simulations. This indicates that the interface element used to model the bar-matrix interaction accurately represented the expected pull-out behavior for the bar in this test.

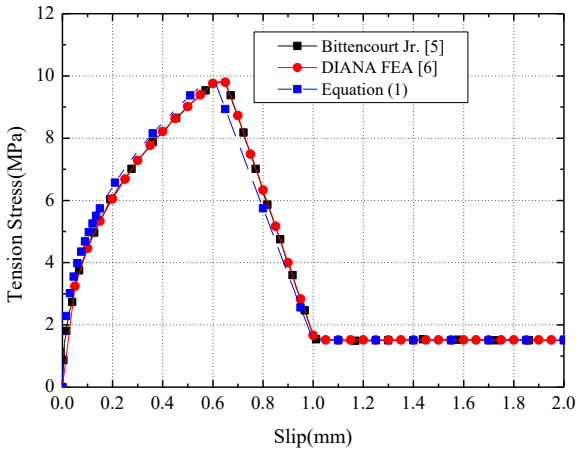


Figura 3 – Rebar stress versus Slip relationship for the computational test A.

Figure 4 presents the results of the simulation for Test B, which focuses on the influence of the fiber embedment length. In the graph, the black curves represent the results obtained using the DIANA FEA® [6] software, while the red and blue curves represent the results from the simulations by Bittencourt Jr. [5] and the results from the analytical DEM (Diverse Embedment Model) [4], respectively.

From these results, it is observed that the fiber embedment length (Xf) influences the maximum tensile stress of the fiber measured at the crack opening. There is a directly proportional relationship between the maximum tensile stress in the fiber and the embedment length (Xf). Furthermore, the maximum tensile stresses in the fibers occur at different crack openings. For Xf equal to 3 mm, the maximum tensile stress was 60.8 MPa for a crack opening of 0.12 mm, while for Xf = 15 mm, the tensile stress and crack opening values were 297 MPa and 0.23 mm, respectively.

The results also show that the responses obtained with the DIANA FEA® [6] software more closely approximated the responses of the analytical Diverse Embedment Model [4] for smaller embedment lengths (Xf) (3, 6, and 9 mm). On the other hand, when adopting larger embedment lengths (12 and 15 mm), the plateaus of these two curves diverge, with the DIANA FEA® [6] results showing lower maximum tensile stress values. The relative difference found between the tensile stresses obtained from the DIANA FEA® [6] simulations and those obtained by Bittencourt Jr. [5] ranged from 69.76% to 92.93% when all fiber embedment lengths are considered, with the largest differences observed for the smallest embedment lengths.

Finally, it is observed that, as in the simulations by Bittencourt Jr. [5], the results from the DIANA FEA® [6] software showed a constant plateau of tensile stress in all simulations, indicating the fiber's pull-out from the matrix before yielding. A slightly different behavior was obtained from the analytical Diverse Embedment Model [4], which showed a slight decay after the maximum tensile stress.

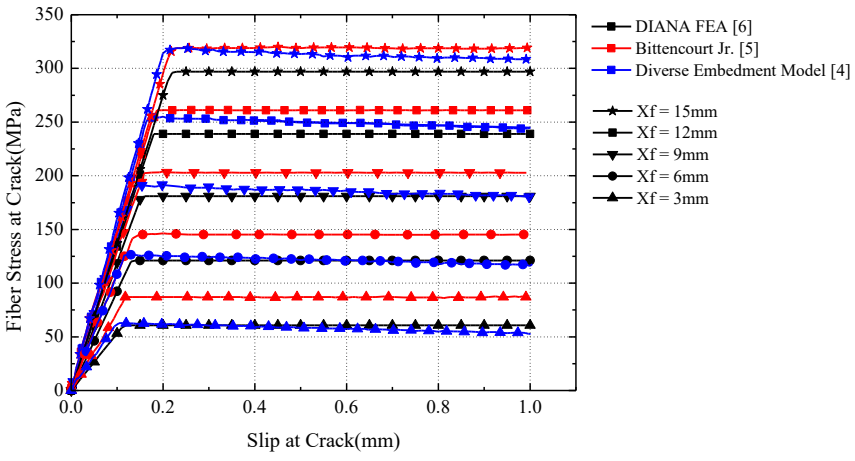


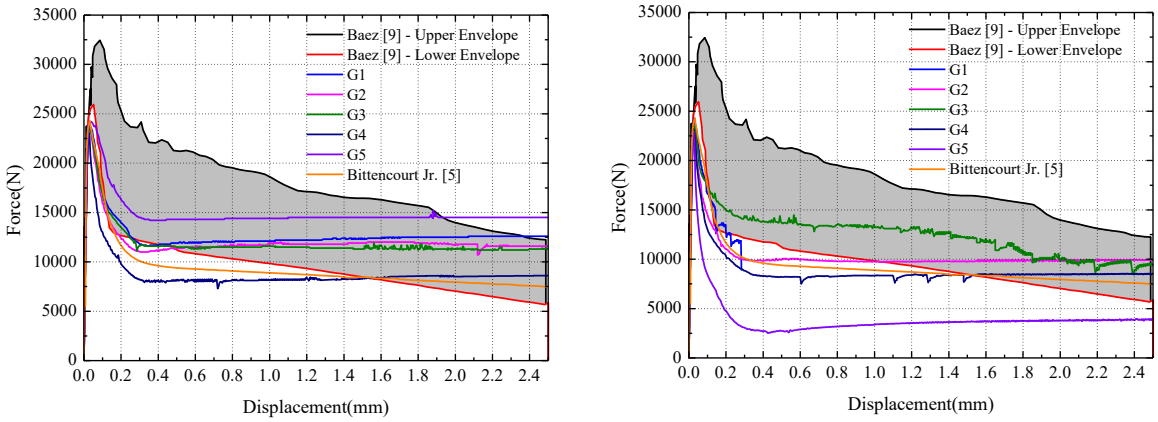
Figure 4 – Fiber tension stress at crack versus slip at crack from the computational test B.

Figure 5 shows the force versus displacement curves obtained from the computational modeling of Test C, which are compared with the region that delimits the experimental responses obtained by Baez [9]. For this modeling, five different fiber generations were performed to identify the influence of the randomness of the dispersed fiber generation in the matrix. The responses obtained for each generation are represented by curves G1 to G5 in figure 5. The result of the numerical simulation performed by Bittencourt Jr. [5] is also presented in the graphs of figure 5.

In general, it is observed that the strategy of allowing or not allowing fiber intersection during generation directly influences the post-peak response of the computational model. In the elastic phase, the responses of the numerical simulations are similar and show good convergence with the experimental results. The maximum forces obtained in the numerical simulations are at the lower limit of the experimental response region.

In the post-peak region, the curves obtained by allowing fiber intersection show higher residual stresses when compared to the responses of the model without allowing intersection, as shown in figures 5a and 5b, respectively. In this analysis, the curves obtained by allowing fiber intersection in the generation show post-peak responses within the region of the experimental responses. The lower residual strength observed in the models without allowing fiber intersection is due to the tendency for these fibers to concentrate at the edges of the central region of the specimen, as shown in figure 2c. This phenomenon also increased the dispersion among the five different fiber generations.

At a crack opening of 0.5 mm, the residual force obtained from figure 5a varied between 8070 and 14300 N, while in figure 5b, the residual force varied between 2740 and 13700 N. In the experiment, the force varied between 11150 and 24171 N for a crack opening of 0.5 mm.



a) Intercepting Fibers – 0,5% Fibers

b) Non-Intercepting Fibers – 0,5% Fibers

Figure 5 – Force versus displacement curves for the computational test C.

5 Conclusions

Modeling FRC is a task that requires attention to several factors. The definition of the bond-slip law for the fiber-matrix interface directly influences the results of the numerical simulation of fiber-reinforced concrete. The models that represented the behavior of only a single fiber showed good agreement with the theoretical bond-slip curves, which indicates that the fiber-matrix interface parameters were correctly defined.

When analyzing the fiber embedment length, it was observed that the pull-out force increased with the embedment length. The computational model developed in DIANA FEA® tended to provide lower pull-out force values than the analytical model as the embedment length increased. Compared to the model developed by Bitten-

court Jr. [5], the pull-out force obtained in the DIANA FEA® software was also lower, which is due to the representation adopted by Bittencourt Jr. [5] for the embedded fiber. By using an interface element at the fiber-matrix interface, one tends to have lower pull-out force values.

Another factor that influenced the results was the consideration of fiber intersection during the generation process. In this case, the post-peak responses that were closest to the experimental results were obtained when fiber intersection was allowed during their generation. In addition, less dispersion of results was observed when five different fiber generations were performed, due to the better uniformity of the fiber distribution in this case.

Acknowledgments. This work was supported by the Coordination for the Improvement of Higher Education Personnel - Brazil (CAPES) - Finance Code 001 and the National Council for Scientific and Technological Development (CNPq) [grant number 305622/2023-4].

Authorship statement. The authors hereby confirm that they are the sole liable persons responsible for the authorship of this work, and that all material that has been herein included as part of the present paper is either the property (and authorship) of the authors, or has the permission of the owners to be included here.

References

[1] Khaloo, Ali R.; Kim, Nakseok. Influence of concrete and fiber characteristics on behavior of steel fiber reinforced concrete under direct shear. Materials Journal, v. 94, n. 6, p. 592-601, 1997.

[2] Ahmed, Tamjeed; Chidambaram, R. Siva. Shear strength of steel fiber reinforced concrete beam–A review. Materials Today: Proceedings, v. 64, p. 1087-1093, 2022.

[3] Lee, G. G.; Foster, S. J. Modelling of shear-fracture of fibre-reinforced concrete. In: Tailor made concrete structures, fib symposium, Amsterdam, The Netherlands. 2008. p. 19-22.

[4] Lee, Seong-Cheol, Jae-Yeol Cho, and Frank J. Vecchio. "Diverse embedment model for steel fiber-reinforced concrete in tension: Model development." *ACI materials Journal* 108.5 (2011): 516.

[5] Bittencourt Jr, Luís A.G. et al. Numerical modeling of steel fiber reinforced concrete with a discrete and explicit representation of steel fibers. International Journal of Solids and Structures, v. 159, p. 171-190, 2019.

[6] DIANA FEA BV, 2021. DIANA FEA finite element analysis - user's manual 10.5.

[7] Ayad Al-Rumaithi (2025). Generate and Crop Fibers (https://www.mathworks.com/matlabcentral/fileexchange/122097-generate-and-crop-fibers), MATLAB Central File Exchange. Retrieved August 1, 2025.

[8] CORNELISSEN, H. A. W., HORDIJK, D. A., AND REINHARDT, H. W. Experimental determination of crack softening characteristics of normalweight and lightweight concrete. *Heron 31*, 2 (1986).

[9] Fabian Augusto Lamus Baez. Modelo numerico del comportamiento inelástico del concreto reforzado con fibras cortas de acero. PhD thesis, Universidad Nacional de Colombia, 2014.